ELSEVIER

Carbohydrate Research 313 (1998) 165–174

CARBOHYDRATE RESEARCH

Structure of the enzymatically synthesized fructan inulin

A.G. Heyer [a,*], B. Schroeer [a], S. Radosta [b], D. Wolff [c], S. Czapla [c], J. Springer [c]

[a] *Max-Planck-Institut für Molekulare Pflanzenphysiologie, Karl-Liebknecht-Str. 25, 14476 Golm, Germany*
[b] *Fraunhofer-Institut für Angewandte Polymerforschung, Postfach 126, 14504 Teltow, Germany*
[c] *Technische Universität Berlin, FG Makromolekulare Chemie, Str. des 17. Juni 135, 10623 Berlin, Germany*

Received 21 April 1998; accepted 10 October 1998

Abstract

Construction, purification and characterization of a fusion protein of maltose-binding protein of *Escherichia coli* and the fructosyltransferase of *Streptococcus mutans* is described. With the purified protein, in vitro synthesis of inulin was performed. The obtained polysaccharide was characterized by high-performance size-exclusion chromatography (HPSEC) and static light scattering (SLS) in dilute aqueous and dimethyl sulfoxide solution. For all samples very high molecular weights between 60×10^6 and 90×10^6 g/mol and a remarkable small polydispersity index of 1.1 have been determined. Small root-mean-square radii of gyration point to a compact conformation in dilute solution. No difference between native and enzymatically synthesized inulin was observed by X-ray powder diffraction and thermoanalysis of solid samples.

Keywords: Fructosyltransferase; *Streptococcus mutans*; Inulin; Light scattering

1. Introduction

Fructans are carbohydrate polymers consisting of a sucrose molecule that is elongated by a chain of fructosyl units connected through β-(2→1) or β-(2→6) linkages (for review, see [1,2]). Depending on the linkage type they are called inulin and levan, respectively.

In nature, fructans occur in bacteria, fungi and plants, serving different functions. In monocotyledonous plants, fructans from the levan type are short-term carbohydrate storage forms in the stem and leaf sheaths that are degraded at later stages of the growth season to provide carbohydrate for grain filling [3]. In most fructan producing dicotyledonous plants, inulin is a long-term storage carbohydrate replacing starch, which is the most common storage carbohydrate in plants. In plants, at least two different enzymes are involved in fructan synthesis, one of which produces the trisaccharide kestose that is substrate to the reaction of the second enzyme [4,5]. Fructans synthesized by plants are mixtures of molecules having different degrees of polymerization (DP), but are usually of low molecular weight ($< 35{,}000$ g/mol; [6]).

Fructans synthesized by bacteria are high-molecular-weight polymers and in almost all cases of the levan type [7]. The only bacterial species known so far that produces an inulin type fructan is *Streptococcus mutans*, a human pathogen involved in dental caries [8]. Although it is well established that extracellular water-insoluble glucans play a role in adhesion of the bacterium to the tooth surface, it is not clear whether the fructose polymer is involved in infection.

* Corresponding author. Tel. +49-331-9772786; fax +49-331-9772301; e-mail: heyer@mpimp-golm.mpg.de

0008-6215/98/$ - see front matter
PII: S0008-6215(98)00281-X

Investigations on the structure of the inulin have revealed that it has a molecular weight of more than 10^6 g/mol [9] and contains not more than 5% β-(2→6)-linked branches [10]. A water-soluble polymer of high molecular weight could be an interesting raw material for industrial purposes such as production of surfactants.

The fructosyltransferase (FTF) gene of *S. mutans* GS-5 has been cloned by metabolic complementation of an *Eschericha coli* strain defective in sucrose metabolism [11]. The FTF gene consists of an open reading frame of 2391 bp and contains a signal sequence of 102 bp that encodes a secretory signal peptide [12].

We have cloned the coding region of the mature peptide as a fusion to the *E. coli* maltose binding protein (MBP) gene to express a fusion protein in *E. coli* that allows purification by amylose affinity chromatography.

With the purified protein we performed in vitro synthesis of high-molecular-weight inulin and studied the enzymatic properties of the fusion protein. The in vitro synthesized polymer was characterized by high-performance size-exclusion chromatography (HPSEC), static light scattering (SLS) in dilute aqueous and dimethyl sulfoxide solution, X-ray powder diffraction and thermoanalysis.

Since light scattering yields absolute values for molecular parameters like weight-average molecular weight, root-mean-square radius of gyration and second osmotic virial coefficient, our size-exclusion chromatography system, equipped with light scattering sensitive detectors, allowed determination of the absolute molecular size of the in vitro synthesized inulin by HPSEC.

2. Results and discussion

Characterization of the MBP–FTF fusion protein.—MBP–FTF fusion protein was purified as described in Section 3. The crude extract of the *E. coli* culture, flow through of the amylose column, and eluate were subjected to sodium dodecylsulfate polyacrylamide gel electrophoresis (SDS-PAGE) to demonstrate the purity of the preparation (Fig. 1).

The eluate consists to at least 90% of a 130,000 g/mol protein species that matches the expected size of the MBP–FTF fusion. Purity of the protein was assessed by densitometric scanning of polyacrylamide gels stained with Coomassie Brilliant Blue dye. The identity of the purified protein as an inulinsucrase was confirmed by incubating 0.1 mg/mL of the protein with 600 mM sucrose for 12 h at 25 °C as described in Section 3. A carbohydrate polymer was synthesized that could be precipitated from the reaction mixture with four volumes of ethanol (80% final concentration). The precipitate was dissolved in hot water and analyzed by TLC (Fig. 2, FTF-reaction product, lane 1). Beside traces of sucrose, kestose and nystose, a fructose-containing substance could be detected that did not migrate with 87:13 acetone–water and should therefore have a DP > 7. A total of 100 μg of the substance dissolved in 100 μL of 50 mM sodium acetate, pH 4.8, could be partially degraded by exo-inulinase (lane 2) and endo-inulinase (lane 3) at 56 °C within 30 min and yielded fructose and a mixture of fructose and oligofructans, respectively.

The combined action of exo- and endo-inulinase completely degraded the substance within the incubation period (lane 4). An equivalent amount of levan from *Erwinia herbicola* was barely degraded by the inulinases (Levan, lanes 1–4). Enzymatic determination

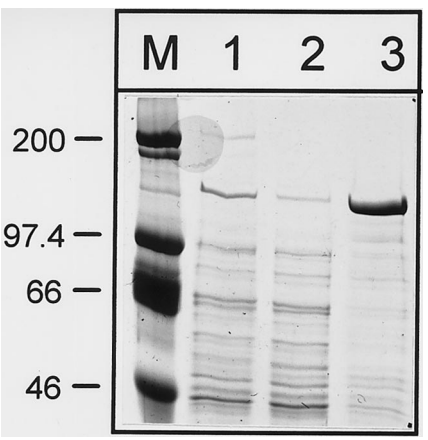

Fig. 1. Sodium dodecylsulfate polyacrylamide gel electrophoresis (SDS-PAGE) of crude extract (line 1) of *E. coli* transformed with the plasmid pMBP–FTF, flow through of chromatography on an amylose resin (lane 2), and eluate of the column (lane 3). A total of 5 μg of protein were loaded on each lane. Molecular weights of marker protein (line M) are given in kDa on the left.

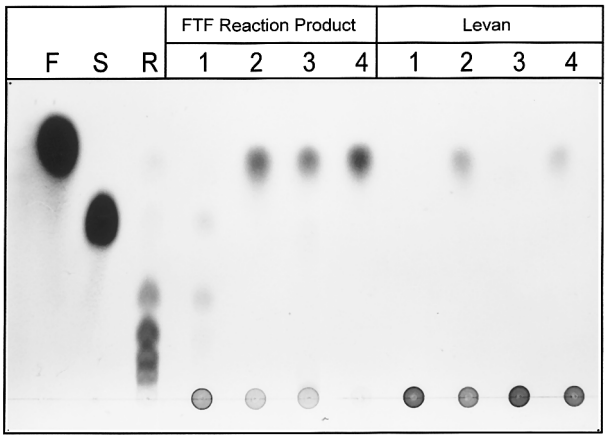

Fig. 2. TLC analysis of the carbohydrate polymer synthesized by the MBP–FTF fusion protein (FTF reaction product) in comparison to levan isolated from *Erwinia herbicola* (levan). Lane 1: untreated polymer; lane 2: degradation by exo-inulinase; lane 3: degradation by endo-inulinase; lane 4: degradation by combined endo- and exo-inulinase. F, fructose standard; S, sucrose standard; R, mixture of fructosyl oligomers, degree of polymerization ranging from 3 to 7.

(see Section 3) of fructose released from both carbohydrate polymers by exo- and endo-inulinase in combination (Fig. 2, FTF-reaction product vs. levan, lane 4) yielded 116.5 μg of fructose for the inulin degradation assay. This corresponds to 104.8 μg of inulin present in the assay. In the case of levan, 16.4 μg of fructose were released, corresponding to 15% of the levan that was incubated with the inulinases. This indicates that the carbohydrate polymer formed by the MBP–FTF fusion protein consists of fructose mainly connected via β-(2→1) linkages.

To define the optimal conditions for in vitro inulin synthesis, we tested various buffer systems, pH values, temperatures and substrate concentrations (Table 1). We found that the pH optimum for the enzyme was 5.4 for incubation times shorter than 20 min. When incubation times were extended to achieve a higher yield of polymer, a pH of 7.2 gave a better result: in a time course over 1080 min, 1359 μmol glucose per mg protein at pH 7.2, but only 956 μmol glucose per mg protein at pH 5.6 were released in a reaction with 100 mM sucrose at room temperature. From the results displayed in Table 1 we determined standard conditions for in vitro inulin synthesis by MBP–FTF (see Section 3).

Solid state properties.—Wide-angle X-ray diffraction on powder samples at ambient temperatures as well as simultaneous differential scanning calorimetry (DSC) and thermogravimetry (TG) were performed to compare enzymatically synthesized samples with native inulin products obtained from dahlia, Jerusalem artichoke and chicory.

On the X-ray diffractograms of enzymatically synthesized polymers, nine or ten reflec-

Table 1
Variation of buffer systems, pH value, substrate concentration and temperature to define the optimal conditions for in vitro inulin synthesis

pH (Na–citrate)	5.2	5.4	5.6	5.8	Experimental
Glucose (μmol/mg min)	8.93 ± 0.14	9.55 ± 0.28	9.15 ± 0.17	8.79 ± 0.24	100 mM sucrose, 25 °C, 0.01 mg/mL protein, 10 mM Na–citrate
Buffer, pH 5.6	Phosphate –citrate	Na–acetate	Citrate –NaOH	Na–phosphate	
Glucose (μmol/mg min)	8.52 ± 0.52	9.65 ± 0.45	8.29 ± 0.39	9.67 ± 0.98	100 mM sucrose, 25 °C, 0.01 mg/mL protein, 10 mM buffer, pH 5.6
Sucrose (mM)	10	100	500	1000	
Glucose (μmol/mg min)	4.81 ± 0.16	9.48 ± 0.64	17.58 ± 0.24	23.09 ± 3.71	25 °C, 0.01 mg/mL protein, 10 mM Na–citrate, pH 5.6
Temperature (°C)	25	28	30	37	
Glucose (μmol/mg min)	7.45 ± 0.25	8.21 ± 0.78	8.31 ± 0.39	7.74 ± 0.56	100 mM sucrose; 0.01 mg/mL protein, 10 mM Na–citrate, pH 5.6

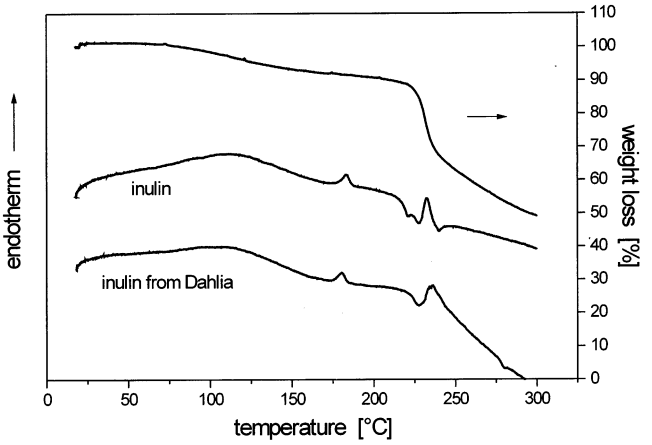

Fig. 3. DSC and TG traces for enzymatically synthesized inulin and inulin obtained from dahlia, heating rate: 10 K/min.

tions already described for native inulin [13,14] were detected. According to these authors, depending on the modification of an orthorhombic crystal lattice, patterns with nine reflections point to monohydrate (two molecules water per two monomer units) and patterns with ten reflections point to hemihydrate (one molecule water per two monomer units) arrangement.

As expected, no difference for melting behavior and thermal stability was observed. In Fig. 3 the DSC and TG traces for enzymatically synthesized and dahlia inulin are shown. A broad endothermic behavior at temperatures between 50 and 150 °C connected with a weight loss of 9% was noticed. Whether this process is connected with release of adsorbed or crystal water is still under investigation. The melting occurred upon further heating at about 180 °C (chicory, 173 °C; Jerusalem artichoke, 175 °C; dahlia, 180 °C; synthesized inulin, 183 °C). For all samples the melting enthalpy was determined to be 8.2 ($\pm$ 0.4) J/g. This process was found to be irreversible and connected with a change of color but no weight loss was observed. At temperatures between 220 and 350 °C degradation leads to a further weight loss of 40%.

Kinetics of inulin synthesis.—The quantity, molecular weight and polydispersity index of inulin synthesized in the batch as a fuction of time were investigated by aqueous size-exclusion chromatography. The area of the chromatogram (normalized to equal injection volume) is related to the concentration of the polymer and shows the increase of inulin quantity as a fuction of time (Fig. 4A,B and Fig. 5). The 600 mM sucrose solution contains a small amount of polymer material (ca. 0.01 mg/mL). This contamination gives the chromatogram for the time at 0 min.

After 4 min the first inulin was detected in the concentration signal and after that a continuous growth of the amount of synthesized inulin could be observed. During the first 20 min the concentration of inulin was too small for molecular weight determination but after that we found an increase of the weight-average molecular weight of the synthesized polysaccharide (Fig. 5). The strongest changes in molecular weight occur during the first 6 h of the reaction time. Between 24 and 48 h, the weight-average molecular weight of the polymer remains constant but the amount of inulin increases further. Very interesting to note is, that the multi angle laser light scattering (MALLS) determined absolute calibration curves shift to higher molecular weights with dependence on the reaction time (Fig. 4A). This means that the density of the synthesized inulin in dilute solution increases with increasing molecular weight. From the chromatograms, no tendency towards aggregation was observed. The polydispersity is very small and seems to be independent of the reaction time. The results are summarized in Table 2 and Fig. 6. Additionally, the values of inulin obtained from a larger batch are given.

Static light scattering (SLS).—The dry polymer, obtained after 14 days of reaction time, is soluble in dimethyl sulfoxide at ambient temperatures and in distilled water at 60 °C. The aqueous solution can be cooled to room temperature without precipitation of the sample.

From Zimm, Berry and Guinier plots the same results were obtained within the experimental error. A typical Guinier plot is shown in Fig. 7 for the system inulin/dimethyl sulfoxide.

For all polymers the same very high weight-average molecular weights of about 70×10^6 g/mol were observed in both solvents. The values of the z-average root-mean-square radius of gyration of 48 nm for inulin in water

at 33 °C and 55 nm for the same inulin in dimethyl sulfoxide at 25 °C are small with respect to the high molecular weight of this polysaccharide. The somewhat higher radius of gyration in dimethyl sulfoxide may indicate a higher degree of swelling of the inulin in dimethyl sulfoxide. From the second osmotic virial coefficients A_2, however, no significant differences between water and dimethyl sulfoxide can be derived.

As can be seen from Table 3, with static light scattering and HPSEC the same M_w values were determined. Also the radius of gyration for an aqueous solution of inulin agrees for both methods. However, for the system inulin/dimethyl sulfoxide, a much higher value was obtained by HPSEC. Taking into account that the SEC measurements were performed at higher temperatures compared to SLS investigations, it is assumed that the thermodynamic quality of the solution does not change with increasing temperature in the system inulin/water but in the system inulin/dimethyl sulfoxide. To prove this, further

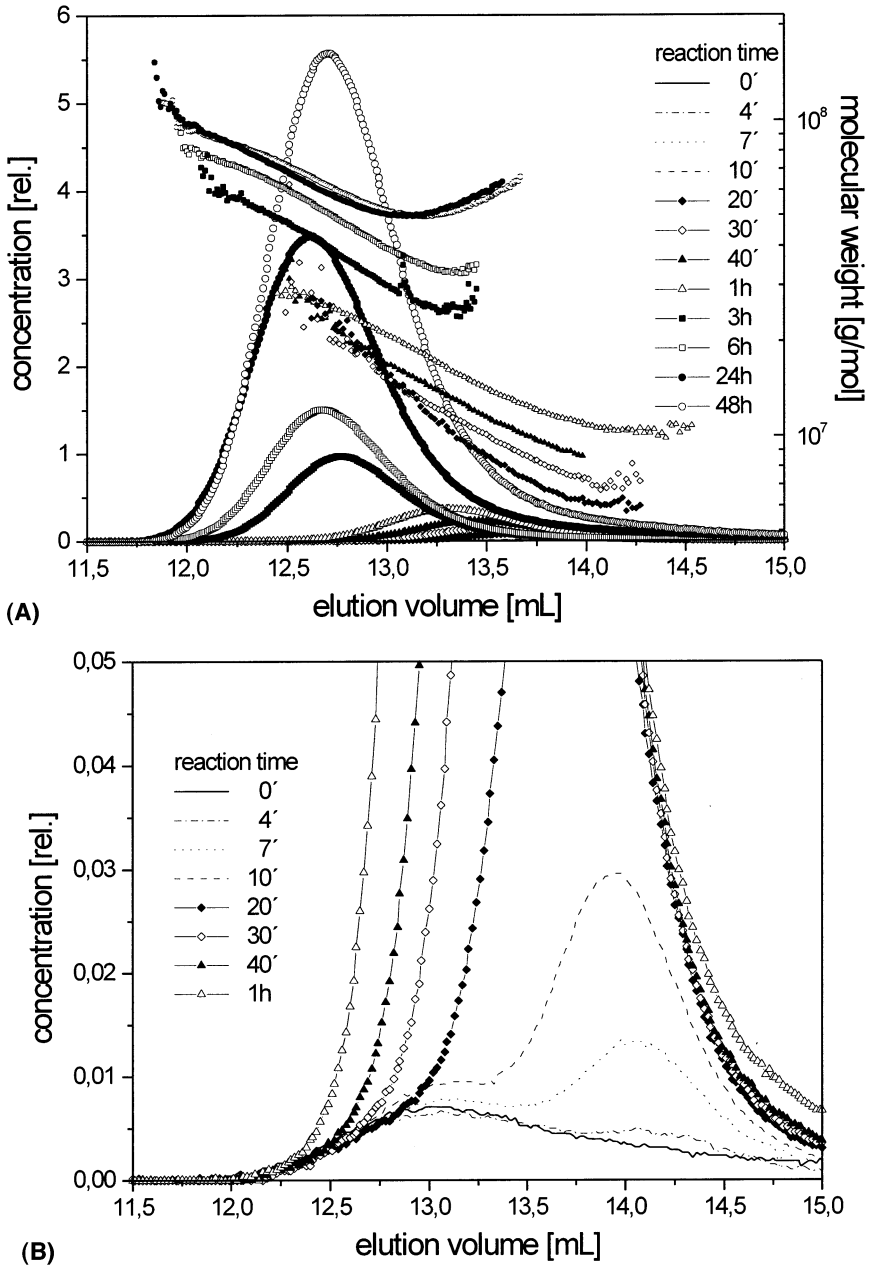

Fig. 4. High-performance size-exclusion chromatograms of synthesized inulin. A: dependence on reaction time; B: enlargement of the small concentration region of (A).

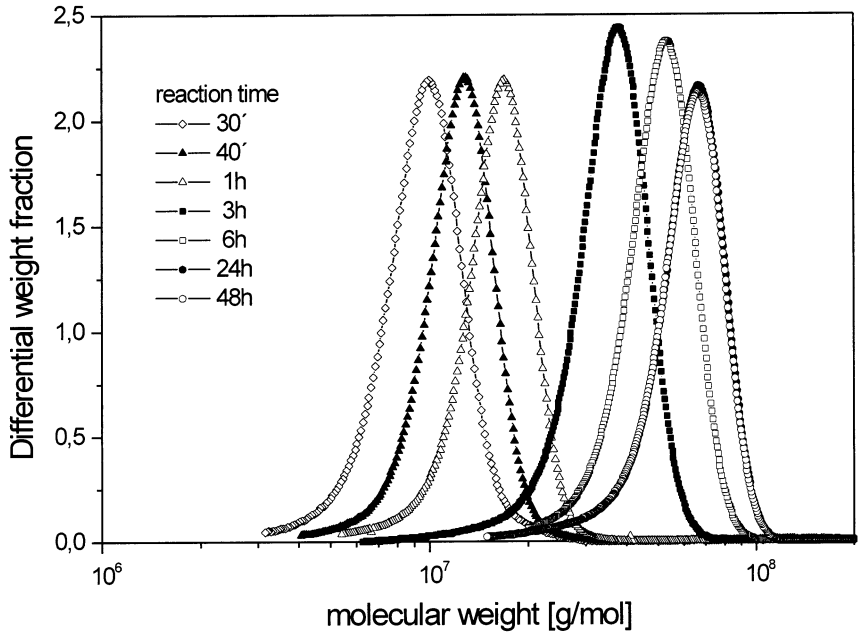

Fig. 5. Molecular weight distribution of synthesized inulin as a function of reaction time.

static light scattering experiments in dependence on temperature are in progress.

Nevertheless, in both solvents the values for the radius of gyration are very small with respect to the high molecular weight of this polysaccharide. This suggests that the molecules assume a compact conformation in both solvents. A compact globular conformation has usually been observed for highly branched levan [15,16]. For high-molecular-weight inulin samples (M_w: $0.1–5.29 \times 10^6$ g/mol) Kitamura et al. assumed a compact conformation from viscometry measurements [17]. This unexpected result was related to strong intramolecular interactions between more distant residues of the same molecule. Our observation, determined by HPSEC, that the structure of the synthesized inulin becomes more and more dense with increasing molecular weight seems to support the assumption of these authors. But also an increasing amount of β-(2→6)-linked branches may be taken into account.

To characterize the shape of the enzymatically synthesized inulin in solution, viscometry, dynamic light scattering in dilute solution and the extension of SLS measurements to a wider concentration region are the subject of continuing investigation. Furthermore, the determination of the amount of β-(2→6)-linked branches is in progress.

3. Experimental

Construction of plasmid pMBP–FTF.—On the basis of general rules for the determination of signal peptides, Shirozawa and Kuramitsu [12] assigned a putative cleavage site for a signal peptidase to Val-34 in the FTF peptide.

Table 2
Weight-average molecular weight, polydispersity index and polymer concentration of synthesized inulin in the batch as a function of time

Reaction time	M_w (10^6 g/mol)	M_w/M_n	Polymer concentration in the reaction mixture (mg/mL)
0			(0.010)[a]
4 min			0.002
7 min			0.011
10 min			0.027
20 min			0.081
30 min	10.5	1.10	0.143
40 min	13.3	1.12	0.214
1 h	17.4	1.13	0.304
3 h	40.1	1.11	0.950
6 h	52.6	1.09	1.509
24 h	65.6	1.08	3.532
48 h	64.0	1.06	5.573
12 days[b]	71.0	1.07	14.2

[a] Polymer comes from sucrose.
[b] Results from a different experiment, inulin concentration determined from yield.

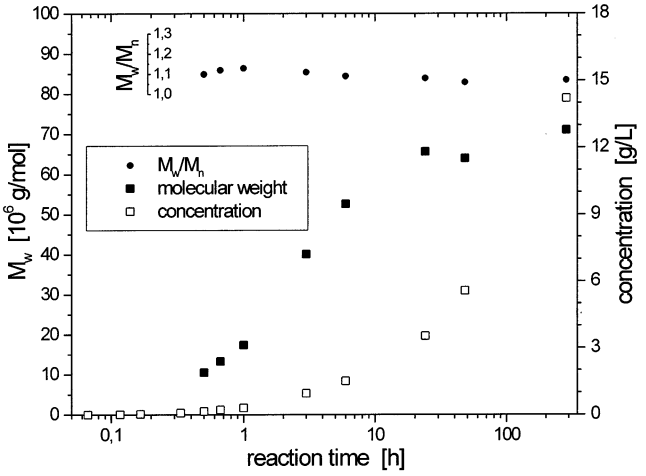

Fig. 6. Weight-average molecular weight, polydispersity and concentration of synthesized inulin as functions of reaction time.

In the FTF gene, a unique *Ear*I restriction site directly precedes the codon for Val-34. To construct a chimeric gene coding for a fusion protein of the *E. coli* MBP and the mature FTF peptide, we cut out the *Ear*I/*Bgl*II restriction fragment of the plasmid pTS102 [12] spanning nucleotides 780 to 3191, blunted the *Ear*I site by filling in the overhanging 5′ end with T4-polymerase and cloned it in the *Cla*I (blunted)/*BamH*I site of pBLUESCRIPT KS (Stratagene GmbH, Heidelberg, Germany), yielding an in frame LacZ fusion. Expression of a functional FTF enzyme was tested by analysis of sucrase activity in protein extracts of bacterial cultures induced by isopropyl β-D-thiogalactoside (IPTG). From this construct, a *Sal*I (blunted)/*Xba*I fragment was cloned into the *Xmn*I/*Xba*I cut vector pMAL-C2 (New England Biolabs GmbH, Schwalbach, Germany) to give pMBP–FTF.

Purification of MBP–FTF by amylose affinity chromatography.—Purification of the MBP–FTF fusion protein was performed as follows. *E. coli* transformed with pMBP–FTF were grown in YT medium to an optical density of $OD_{600} = 0.6$ at 37 °C. Expression of the fusion protein was induced by adding 1 mM IPTG and extending culture for 2 h. After cooling in ice water, cells were harvested by centrifugation at 3000 min^{-1} in a Beckman GS-6KR centrifuge. The cell pellet was resuspended in 10 mM Na_2HPO_4/NaH_2PO_4, pH 7.2, 30 mM NaCl, 10 mM (ethylenedinitrilo) tetraacetic acid disodium salt (EDTA), 10 mM [ethylenebis (oxyethylenenitrilo)] tetraacetic acid (EGTA), 10 mM 2-mercaptoethanol and cells were lysed by one passage through a precooled french pressure cell (SLM Aminco, SLM Instruments, Rochester, NY) at 2500 psig. The lysate was adjusted to 500 mM NaCl and loaded onto an amylose resin (New England Biolabs GmbH, Schwalbach, Ger-

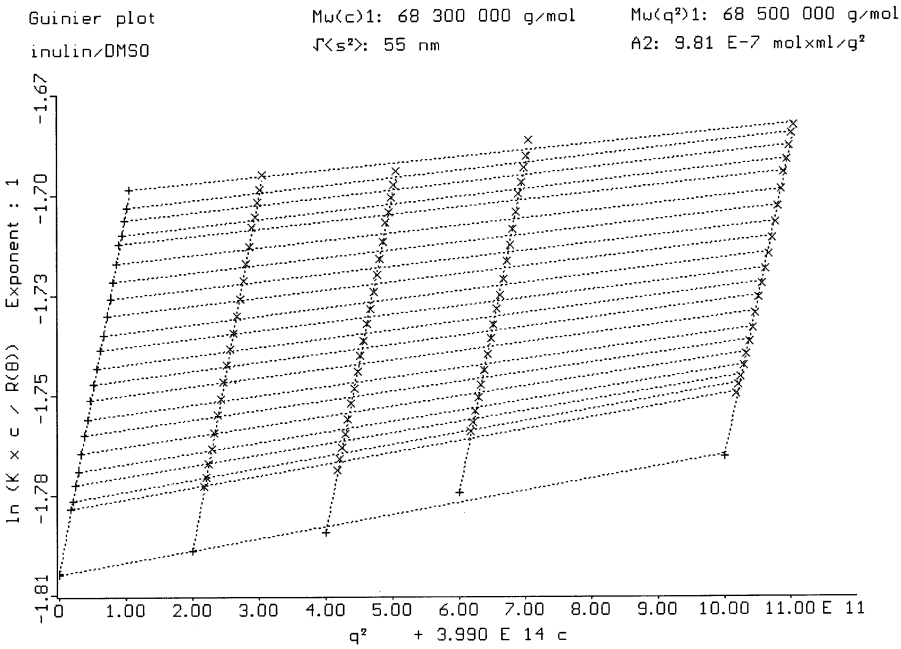

Fig. 7. Guinier plot of inulin in Me_2SO at 25 °C, concentration: 0.5014 g/L; 1.0029 g/L; 1.5043 g/L; 2.5070 g/L.

Table 3
Comparison of weight-average molecular weight M_w and z-average root-mean-square radius of gyration obtained by HPSEC and SLS

	M_w (10^6 g/mol)	M_w/M_n (from HPSEC)	Radius of gyration (nm)
Inulin–water	HPSEC: 71, SLS: 71	1.07	HPSEC: 47 (75 °C), SLS: 48 (33 °C)
Inulin–Me_2SO	HPSEC: 70, SLS: 68	1.11	HPSEC: 76 (60 °C), SLS: 55 (25 °C)

many) at a flow rate of 0.2 mL/min at 4 °C. The column was washed with 10 bed volumes of 10 mM Na_2HPO_4/NaH_2PO_4, pH 7.2, 500 mM NaCl, 1 mM EGTA and the fusion protein was eluted from the column in the same buffer containing 10 mM maltose.

In vitro inulin synthesis.—Synthesis of inulin by MBP-FTF was performed in reaction mixtures containing 600 mM sucrose as substrate and a concentration of 0.1 mg/mL of the fusion protein. The standard condition was 10 mM Na_2HPO_4/NaH_2PO_4, pH 7.2, 1% glycerol, 28 °C. As the protein was eluted in a concentration of 1 mg/mL with 10 mM maltose from amylose resin, reaction mixtures also contained 1 mM maltose. For quantitative conversion of sucrose an incubation time of 14 days was applied. At the end of the synthesis the solution was dropped into EtOH (80% final concentration) The precipitate was filtered and dried to constant weight in vacuum at 40 °C. The polymer was obtained with a yield of 14 wt.% with respect to fructosyl groups of the substrate. For kinetics studies, specimens of the solution were taken in dependence on time and the enzymatic reaction was stopped by addition of 0.1% of sodium dodecylsulfate to the reaction mixture.

Thin-layer chromatography.—Fructose and fructose-containing saccharides were analyzed by TLC on silica gel F1500 (Schleicher & Schuell, Dassel, Germany). 2 μL of 1/10 dilutions of the reaction mixtures were spotted on the plates and developed in 87:13 acetone–water and stained with a fructose-specific urea phosphoric acid spray [18].

Enzymatic determination of glucose and fructose.—Glucose and fructose were measured by the glucose-6-phosphate-dehydrogenase method [19]. Glucose was measured in 100 mM imidazole-HCl (pH 6.9), 5 mM $MgCl_2$, 2 mM nicotinamide adenine dinucleotide phosphate (NADP), 1 mM adenosine triphosphate (ATP), 2 U/mL glucose-6-phosphate-dehydrogenase (from yeast). The reaction was started by adding 1.4 U hexokinase (from yeast), and absorption of NADPH was followed at 340 nm. Fructose was measured by sequential addition of 2.8 U phosphoglucoisomerase (from yeast).

High-performance size-exclusion chromatography.—Two different HPSEC systems were applied for the investigation of the molecular weight distribution of inulin samples. One system works with an aqueous salt solution and the other works with Me_2SO as the eluent.

Depending on the polymer concentration, for kinetics studies 20–300 μL of the reaction mixture were analyzed by aqueous HPSEC.

Aqueous eluent. The HPSEC system consisted of a Waters 150CV integrated SEC device with pump, autoinjector, column compartment, differential refractive index detector (DRI) and MALLS detector. The MALLS detector, a Dawn-F-DSP laser photometer (Wyatt Technology, Santa Barbara) was fitted with a K5 flow cell and a He–Ne laser operating at $\lambda_0 = 632$ nm and equipped with 18 detectors at angles ranging from 14.4 to 163°. Two Waters columns Ultrahydrogel linear with a dimension of 300×7.8 mm were used in series. The elution was carried out with 0.05 M aq $NaNO_3$ at a flow rate of 0.545 mL/min and a temperature of 75 °C.

Me_2SO eluent. The HPSEC system (Waters) consisted of a 600MS pump module, 717 autoinjector, column compartment, RI-detector 410, and MALLS detector, a Dawn-F-DSP laser photometer (Wyatt Technology, Santa Barbara) fitted with a S2 flow cell and an Ar-ion laser operating at $\lambda_0 = 488$ nm and equipped with 18 detectors at angles ranging from 7.5 to 157°. The columns were Waters Styragel HMW 7, HMW 6E and HT 3 with a dimension of 300×7.8 mm. The elution of samples was carried out with Me_2SO contain-

ing 0.09 M $NaNO_3$ at a flow rate of 0.5 mL/min and a temperature of 60 °C.

The MALLS detector was serially connected with the refractive index detector (DRI) for both devices. During a sample run on the HPSEC-MALLS system the data from the DRI and MALLS detector were collected and processed to give molecular weight at each retention volume.

Static light scattering.—The measurements were carried out in dilute aqueous and Me_2SO solution at 33 and 25 °C, respectively, using a modified (SLS-Systemtechnik, Hausen i.W., Germany) computer-controlled Fica 50 (Fica, Le Mesnil-Saint Denis, France) equipped with a laser operating at $\lambda_0 = 543.5$ nm. The intensity of scattered light was detected with a photomultiplier at angles ranging from 45 to 145°. The solutions were made dust-free by centrifugation at about $3000 \times g$ for 15 min. The refractive index increments were determined with a differential refractometer according to Asmussen and Springer [20] at 546 nm (inulin–water at 33 °C: 0.1313 cm^3/g; inulin–Me_2SO at 25 °C: 0.0659 cm^3/g).

Evaluation of light-scattering data.—The correlation between scattered light from a diluted macromolecular solution and the molecular weight distribution was formulated by Debye [21] and Zimm [22]:

$$\frac{K \cdot c}{R(q)} = \frac{1}{M_w}\left[1 + \frac{16\pi^2}{3\lambda^2}\langle s^2\rangle_z \sin^2\left(\frac{\theta}{2}\right)\right] + 2A_2 c \quad (1)$$

with

$$K = \frac{4\pi^2 n_0^2}{N_A \cdot \lambda_0^4}\left(\frac{dn}{dc}\right)_T^2$$

where K is the optical constant; n_0 is the refractive index of the solvent; $(dn/dc)_T$ is the refractive index increment; N_A is Avogadro's number; λ is the wavelength of light in solution (λ_0: in vacuum), $R(q)$ is the Rayleigh ratio; $q = (4\pi/\lambda)\cdot\sin(\theta/2)$ is the value of the scattering vector; c is the polymer concentration (g polymer/mL solution); A_2 is the second osmotic virial coefficient; M_w is the weight-average molecular weight; θ is the angle between scattered and incident light; and $\sqrt{\langle s^2\rangle_z}$ is the root-mean-square radius of gyration.

The basis for the absolute characterization of macromolecules by HPSEC–light-scattering experiments was described by Wyatt [23]. Molecular weight and radius of gyration were calculated for each slice of the chromatogram on the basis of Eq. (1) using the ASTRA 4.2 software. For every slice of the chromatogram the scattered light is measured as a function of scattering angle with the MALLS detector and the concentration is measured with the refractive index detector. As a result for every slice i an absolute molecular weight M_i can be calculated so that one gets an absolute calibration curve for each sample. The molecular weight distribution curve is calculated using the refractive index signal and the absolute calibration curve.

From the SLS measurements the weight-average molecular weight M_w, the z-average root-mean-square radius of gyration $\sqrt{\langle s^2\rangle_z}$ and the second osmotic virial coefficient A_2 were determined according to the extrapolation method $q \to 0$ and $c \to 0$ given by Zimm [24] using the SLS 4.2 software by SLS-Systemtechnik, Germany. Because of high molecular weight and small gyration radius not only the Zimm-plot: $K \cdot c/R(q)$ versus $\sin^2(\theta/2) + k \cdot c$ but also the Berry-plot: $\sqrt{K \cdot c/R(q)}$ versus $\sin^2(\theta/2) + k \cdot c$ and the Guinier-plot: $\ln \sqrt{K \cdot c/R(q)}$ versus $\sin^2(\theta/2) + k \cdot c$ were used.

Thermoanalysis.—The thermal behavior of inulin was investigated by simultaneous DSC and TG on a Rheometric scientific STA 1000 apparatus between 25 and 350 °C in an oxygen gas flow (50 cm^3/min). For each experiment, 5 mg of sample were put in an aluminum pan and heated with a rate of 10 K/min.

X-ray diffraction.—Wide-angle X-ray diffraction was performed on powder samples at ambient temperatures. Nickel filtered Cu–Kα radiation ($\lambda = 0.154$ nm) was focused by a glass capillary. The patterns were detected with a flat film camera.

Acknowledgements

Financial support of this work (project no.: 0311135) by the Bundesministerium für Bildung, Wissenschaft, Forschung und Technologie, Germany, is gratefully acknowledged.

References

[1] A.D. French, *J. Plant Physiol.*, 134 (1989) 125–136.
[2] C.J. Pollock, *New Phytol.*, 104 (1986) 1–24.
[3] C.J. Pollock, A.J. Cairns, *Annu. Rev. Plant Physiol. Plant Mol. Biol.*, 42 (1991) 77–101.
[4] M. Lüscher, C. Erdin, N. Sprenger, U. Hochstrasser, T. Boller, A. Wiemken, *FEBS Lett.*, 385 (1996) 39–42.
[5] W. Van den Ende, A. Van Laere, *Planta*, 200 (1996) 335–342.
[6] W. Praznick, R.H.F. Beck, *J. Chromatogr.*, 348 (1985) 187–197.
[7] G.L. Cote, J. Ahlgren, in M. Suzuki, J. Chatterton (Eds.), *Science and Technology of Fructans*, CRC Press, Boca Raton, FL, 1993, pp. 192–223.
[8] W.J. Loesche, *Microbiol. Rev.*, 50 (1986) 353–380.
[9] S. Ebisu, K. Kato, S. Kotani, A. Misaki, *J. Biochem.* (*Tokyo*), 78 (1975) 879–887.
[10] K.G. Rosell, D. Birkhed, *Acta Chem. Scand. B*, 28 (1974) 589.
[11] S. Sato, H.K Kuramitsu, *Infect. Immun.*, 52 (1986) 166–170.
[12] T. Shiroza, H.K Kuramitsu, *J. Bacteriol.*, 170 (1988) 810–816.
[13] R. Marchessault, T. Bleha, Y. Deslandes, J.-F. Revol, *Can. J. Chem.*, 58 (1980) 2415–2422.
[14] I. Andre, K. Mazeau, I. Tvaroska, J.-L. Putaux, W.T. Winter, F.R. Taravel, H. Chanzy, *Macromolecules*, 29 (1996) 4626–4635.
[15] S.S. Stivala, J.E. Zweig, *Biopolymers*, 20 (1981) 605–620.
[16] B.A. Khorramian, S.S. Stivala, *Carbohydr. Res.*, 108 (1982) 1–12.
[17] S. Kitamura, T. Hirano, K. Takeo, M. Mimura, K. Kajiwara, B. Stokke, T. Harada, *Int. J. Biol. Macromol.*, 16 (1994) 313–317.
[18] M. Röber, K. Geider, B. Mueller-Röber, L. Willmitzer, *Planta* (*Heidelberg*), 199 (1996) 528–536.
[19] M. Stitt, R. McLilley, R. Gerhartdt, H.W. Heldt, *Methods Enzymol.*, 174 (1989) 518–552.
[20] F. Asmussen, J. Springer, *Meßtechnik* (*Braunschweig*), 3 (1972) 77–80.
[21] P. Debye, *J. Appl. Phys.*, 15 (1944) 338–342.
[22] Ph.J. Wyatt, *Anal. Chim. Acta*, 272 (1993) 1–40.
[23] Ph.J. Wyatt, *Anal. Chim. Acta*, 272 (1993) 1–40.
[24] B.H. Zimm, *J. Chem. Phys.*, 16 (1948) 1093–1099.